

## 3D PRINTING OF SUPER CONCENTRATED ALGINATE CLAY INK WITH POTENTIAL APPLICATION IN REGENERATIVE MEDICINE

Rebeca LEU ALEXA<sup>1</sup>, Horia IOVU<sup>2\*</sup>, Madalina Cristina NICOLAE<sup>3</sup>, Ionut Catalin MIHAESCU<sup>4</sup>, Elvira ALEXANDRESCU<sup>5</sup>, Raluca IANCHIS<sup>6</sup>

*The central objective of this study was to obtain a 3D printable ink with possible application in regenerative medicine. On this line, we developed printable inks based on alginate in a concentration of 5% and ClositeNa (ClNa) in two concentration (18% and 20%).*

*All the ink formulations were characterized from the point of view of printability, then a roundness analyze was performed to quantify the printing fidelity. It could be observed that with the increase of the clay concentration, the structural integrity of the scaffolds was enhanced. Also, all the materials were characterized using FTIR, SEM, TGA and Nanoindentation analysis.*

**Keywords:** alginate, natural clay, 3D printing

### 1. Introduction

Due to the growing need for organs, the field of regenerative medicine is increasingly studied, and the methods used for tissue regeneration are constantly evolving. 3D printing represents one of the main technologies studied in this research field, because it is a non-invasive technology able to manufacture personalized implants. To obtain scaffolds based on biopolymers, these should act like an extracellular matrix. Therefore, in addition to biocompatibility and biodegradability biopolymer-based hydrogels should have adjustable mechanical properties and allow obtaining a structure that respects in detail the design of the

<sup>1</sup> PhD eng., Advanced Polymer Materials Group, Department of Bioresources and Polymer Science, University POLITEHNICA of Bucharest, Romania, e-mail: leurebeca@gmail.com

<sup>2</sup> Prof., Advanced Polymer Materials Group, Department of Bioresources and Polymer Science, University POLITEHNICA of Bucharest, Romania; and Academy of Romanian Scientists, Bucharest, Romania e-mail: horia iovu@upb.ro

<sup>3</sup> MS., Advanced Polymer Materials Group, Department of Bioresources and Polymer Science, University POLITEHNICA of Bucharest, Romania, e-mail: madalina.nicolae15@gmail.com

<sup>4</sup> Eng., National R-D Institute for Chemistry and Petrochemistry ICECHIM—Bucharest, Romania

<sup>5</sup> Eng., National R-D Institute for Chemistry and Petrochemistry ICECHIM—Bucharest, Romania, e-mail: elviraalexandrescu@yahoo.com

<sup>6</sup> National R-D Institute for Chemistry and Petrochemistry ICECHIM—Bucharest, Romania, e-mail: ralumoc@yahoo.com

scaffold [1, 2, 3]. A multitude of bio-inks functioning in 3D printing have been widely studied. Among these we can list gelatin, gelatin methacrylate, alginate, chitosan, polycaprolactone [4, 5, 6].

Alginate is an anionic polysaccharide derived from brown algae and widely consists of two polymer blocks  $\beta$ -(1 $\rightarrow$ 4)-linked d-mannuronic acid (M) and  $\alpha$ -(1 $\rightarrow$ 4)-linked L-guluronic (G) residues. Generally, alginate is easily crosslinked with calcium ions through ionic interactions between  $\text{Ca}^{2+}$  and carboxylic groups present in its structure. Alginate precursor solutions are one of the most studied in regenerative medicine because of cheap cost, biocompatibility and quick gelation [7].

Also, alginate presents a shear thinning behavior, property that recommends it in 3D printing. For example, alginate was used as a matrix for chitosan to obtain a hydrogel usable in tissue regeneration [6]. In another study alginate was employed as drug delivery system [8]. Mahdiyar Shahbazi et al. used alginate intercalated into clay (Cloisite20A) galleries to remove inorganic micropollutants from wastewaters [9]. Two of the main disadvantages of using alginate in 3D printing are low viscosity and low porosity.

It was demonstrated that clay inclusion into the alginate hydrogel strengthens the alginate network providing a high viscosity, property that allows to improve the architecture fidelity of the 3D printed scaffolds [10]. Also, the inclusion of clay in the alginate matrix leads to increased porosity, a property of particular importance for cell attachment and proliferation, leading to tissue regeneration [11-13]. Therefore, the main objective of this research study was to improve the viscosity and porosity of alginate through the introduction of a natural clay. Commercial CloisiteNa clay was used to obtain a printing ink usable in tissue engineering.

Montmorillonite, named also ClositeNa, is a natural clay, its structure consisting in one alumina octahedral sheet placed between two silicon tetrahedral layers with general formula -  $[(\text{Na},\text{Ca})0.33(\text{Al},\text{Mg})_2\text{Si}_4\text{O}_{10}(\text{OH})_2 \cdot n\text{H}_2\text{O}]$ . Montmorillonite is a major component of bentonite and was approved to be used in medicinal products by the Food and Drug Administration (FDA) [14, 15].

The alginate nanocomposites forerunner solution and its crosslinked scaffolds were characterized by Fourier-transform infrared spectrometry (ATR-FTIR) for constitutional characterization, printability for setting the right parameters for ink printing, hydrophilicity was determined by swelling analysis, Scanning Electron Microscopy (SEM) to observe the texture of the scaffolds, nanoindentation to study the mechanical behavior of the nanocomposites obtained after crosslinking process and statistical analyses in order to observe if there are significant differences between the composite hydrogels.

## **2. Materials and Methods**

### **2.1 Materials**

Alginate was purchased from Sigma-Aldrich (Norway), natural montmorillonite with commercial name CloisiteNa (ClNa) was donated by Southern Clay Products Inc. (Gonzales, TX, USA). Ultrapure water and Phosphate buffered saline (PBS) solution pH=7.4 were achieved in our laboratory.

### **2.2 Manufacture of the Alginate based inks**

To achieve the most advantageous composite hydrogel-based inks for the 3D printing process, we selected two concentrations of natural clay (18% and 20% w/w to final solution), and alginate in a fixed concentration of 5% w/v. Modified Alginate was synthesized as further described. Firstly, an alginate solution was obtained by hydrating alginate powder in ultrapure water. After, CloisiteNa powder was added in the alginate viscous solution, mixing gently with a spatula until the clay was homogeneously incorporated.

### **2.3 Fourier-transform infrared spectrometry (ATR-FTIR)**

Constitutional characterization of alginate, CloisiteNa and the nanocomposites obtained was performed using a Fourier-transform infrared spectrometry (Vertex 70 Bruker U.S.A). This FTIR spectrometer is supplied with an attenuated total reflectance (ATR) accessory, and the FTIR spectra were recorded at a resolution of 2 cm<sup>-1</sup> in 4000-400 cm<sup>-1</sup> wavenumber region.

### **2.4 Alginate-based Hydrogels Printability**

To study the printability of alginate and nanocomposites-based inks, 3D Discovery™ printing machine from RegenHU Ltd, Switzerland was used. Materials were printed using a cartridge of 5 ml and cylindrical nozzle of 23G, a printing speed of 4 mm/s and a pressure in the range of 450-505 kPa. The printing process was repeated more than three times. Scaffolds were 3D printed at 25-30°C (depending on the room temperature).

### **2.5 Scanning Electron Microscopy (SEM) Analysis**

The nanocomposite scaffolds which were obtained under 3D printing process, were lyophilized and torn. Then, using Environmental Scanning Electron Microscopy ESEM-FEI Quanta 200, the samples were analyzed as such, without being sputter-coated. Micrographs were taken in vacuum conditions (2 torr) operating at 25–30 KV accelerating voltage using magnifications in the interval of 2000-5000X for rupture area of alginate and nanocomposite samples.

### **2.6 Swelling and dissolvability measurements of the 3D printed scaffolds based on alginate and nanocomposites.**

The hydrophilicity of the alginate and nanocomposite-based scaffolds was determined by measuring the swelling ratios of scaffolds to equilibrium. First, the

residual liquid was removed, and then, the weight of each scaffold was determined [16]. Using the equation 1, the degree of swelling was calculated:

$$\text{Swelling degree (\%)} = \frac{(W_w - W_d)}{W_d} \times 100 \quad (1)$$

Where:  $W_w$  = weight of swollen polymer,  $W_d$  = weight of polymer.

## 2.7 Mechanical properties

Mechanical properties of the crosslinked 3D printed scaffolds were determined using Nano Indenter® G200 (Santa Clara, U.S.A), and a G-Series DCM CSM Flat Punch Complex Modulus, Gel was taken. By this method, storage modulus  $G'$ - and loss modulus- $G''$  of gels are determined very quickly. First, the test is initiated moving the sample under the microscope head. Then, after setting the working parameters, the sample is moved from the microscope under DCM II head. Finally, after all the indentations are performed, the sample is turn automatically under the microscope head.

## 2.8 Thermogravimetry analysis (TGA)

TGA analysis was done on a Q5000 model from TA Instruments. TGA experiments were performed in a nitrogen ambiance with a ejection flow rate of 40.0 mL/min. All samples were loaded one by one in the instrument. At the beginning of each experiment, every sample was loaded into a sample pan in the heating zone of the TGA. Each s was heated to 710°C with an increment of 10°C per minute and kept 5 minutes in isothermal conditions.

## 3. Results

### 3.1 ATR-FTIR

In order to check that alginate was modified with ClositeNa, infrared absorption spectrum of alginate and alginate modified with clay were registered. The specific absorption bands of functional groups from alginate composition were found at 1604  $\text{cm}^{-1}$  (C=O bond) and 1422  $\text{cm}^{-1}$ . The characteristic peaks of CINa were observed at 1040-1048  $\text{cm}^{-1}$  and correspond to Si-O-Si stretching vibration. The next peaks at ~460/520  $\text{cm}^{-1}$  are attributed to Al-Si-O vibration [17, 18] and at ~3400-3600  $\text{cm}^{-1}$  to OH stretching vibration.

FTIR spectrometry confirmed the inclusion of clay in the alginate polymeric matrix by the presence of the specific peaks of alginate and clay that are found in alginate-clay composite sample.

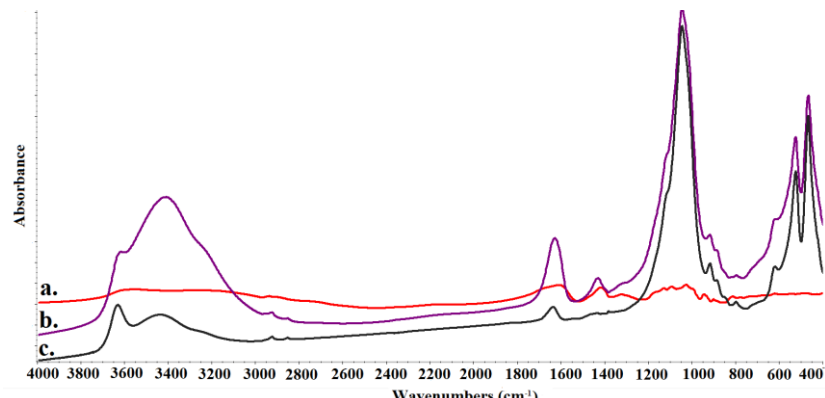


Figure 1. FTIR spectra of a) alginate b) alginate-clay c) clay

### 3.2 Printability and morphology of nanocomposites hydrogels

The main objective of this study was to obtain a printable alginate nanocomposites-based hydrogel paste. In order to investigate the printability of inks and to obtain the best formulation, we pursued the development of suitable alginate nanocomposite inks using different concentrations of clay in the alginate matrix.

Alginate, and alginate-clay hydrogels were printed using a 5 ml cartridge and a needle of 23 G and different pressures in the interval of 450-505 kPa. BIOCAD software was employed to design the scaffold architecture. Printing process was performed at 25-30°C (room temperature). The crosslinking step was accomplished by introducing the printed scaffolds in a calcium chloride solution. First, we tried to print alginate in a concentration of 5% w/v, but the ink was too soft, and the layers collapsed as soon as they were printed. Then, in order to improve the apparent rheological properties, and to obtain a printable hydrogel ink, ClositeNa was added in alginate matrix in two concentrations (18% and 20%). The structural integrity of the filaments obtained with 18% clay was maintained after they encountered the lamella on which were printed but the filaments became larger and spread after printing process (Figure 2b).

At last, alginate with 20% clay was printed. The filaments maintained their structural integrity and the resulted scaffolds presented enhanced stability after the 3D printing process when compared with 18% clay sample (Figure 2b).

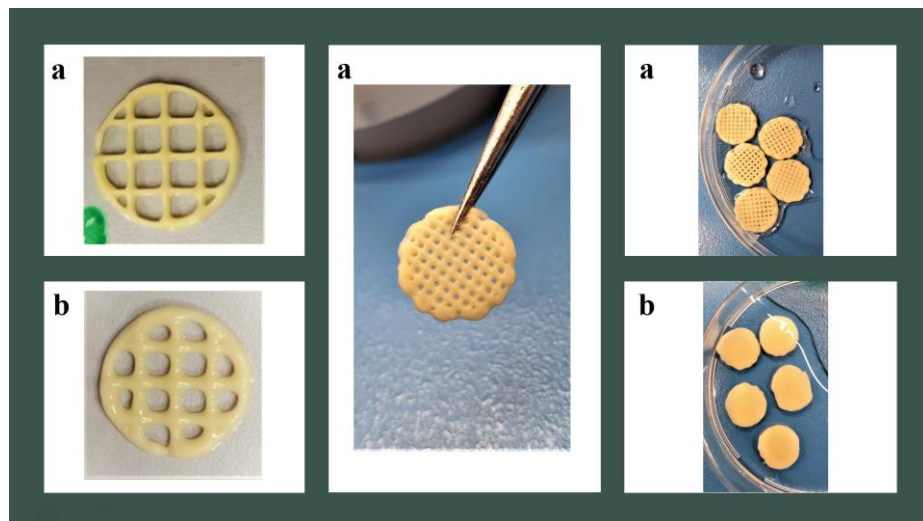


Figure 2. 3D printing process and Printing tests

SEM and EDAX analysis were performed on crosslinked samples to study the porosity and morphology of scaffolds after the crosslinking process. Alginate-based hydrogel presented few pores (Figure 3), but the introduction of clay in the alginate matrix induced a higher porosity (Figure 4 and Figure 5). Both samples, alginate-clay 18% (Figure 4) and alginate clay 20% (Figure 5) presented macropores with different size separated by rough surface walls. Wall surface roughness is one of the most important parameters for scaffolding used in tissue engineering, as roughness improves cell adhesion to scaffold walls. Apparently, clays induce a higher porosity on alginate matrix as a consequence of its interaction with the polymeric matrix [1, 10]. EDAX analysis confirmed the presence of the clay, and  $\text{CaCl}_2$  in alginate matrix (Figure 6).

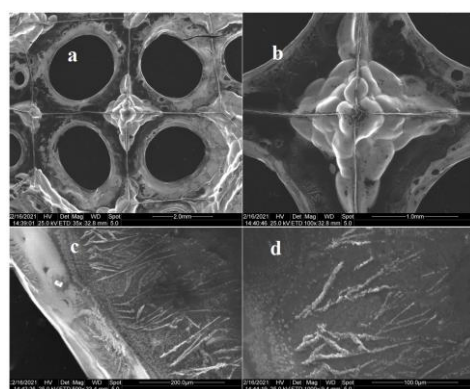


Figure 3. Scanning Electron Microscopy images of alginate at different magnitudes: a) 35X; b) 100X; c) 500X; d) 1000X;

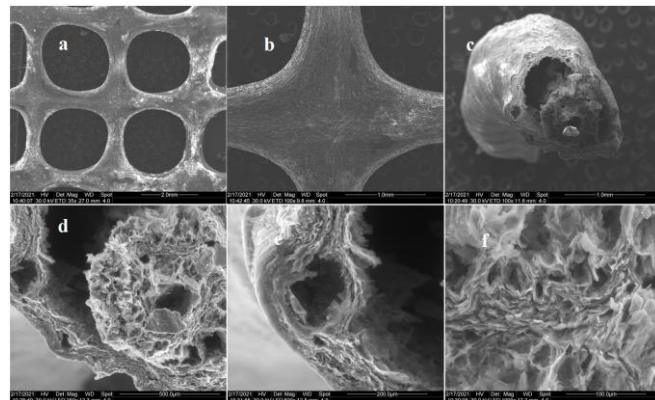


Fig. 4. Scanning Electron Microscopy images of alginate-clay 18% at different magnitudes: a) 35X; b) 100X; c) 100X; d) 250X; e) 500X; f) 1000X)

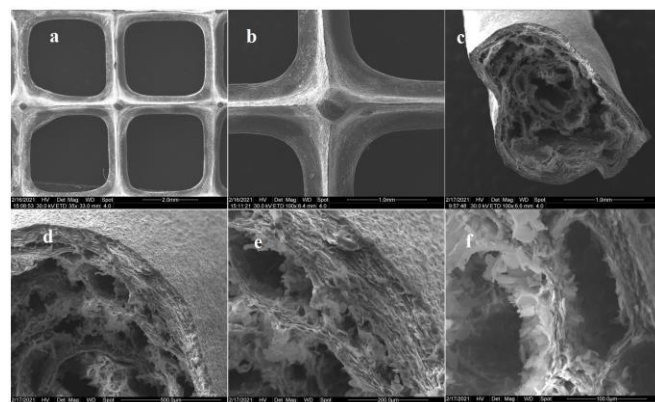


Fig. 5. Scanning Electron Microscopy images of alginate-clay 20% at different magnitudes: a) 35X; b) 100X; c) 100X; d) 250X; e) 500X; f) 1000X)

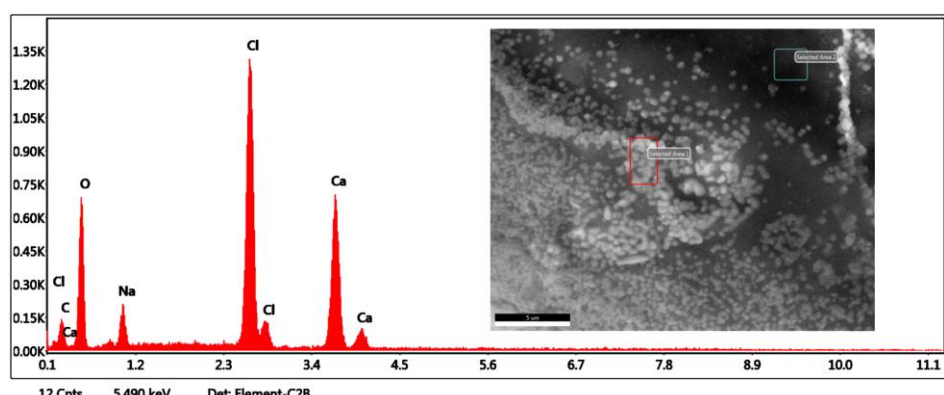


Fig. 6. EDAX analysis on crosslinked samples

In order to quantify the printed shapes, roundness analysis of the open pores was calculated using SEM images and the Wadell equation [19]. To

quantify a perfectly round object, a value of  $R = 1$  is considered, and for irregular objects values  $R < 1$  are attributed.

In our study we obtained a value of  $R = 0.98$  for the alginate matrix,  $R = 0.72$  for 18% alginate-clay and  $R = 0.5$  for 20% alginate-clay. These significant differences indicate that 3D printed scaffolds based on 20% alginate-clay maintained their shape fidelity better than those obtained with 18% alginate-clay and alginate.

### 3.3 Swelling Behavior Studies

Another important parameter worthy to be studied is the hydrophilic/hydrophobic behavior of biopolymers. Usually, the degree of swelling is changed by the concentration of the polymer used, by pore numbers and size. Our research targeted on the influence of clay on the swelling behavior of alginate-based samples. With the introduction of clay in the alginate matrix, the swelling degree decreases. The effect was attributed by the presence of a large amount of clay which does not absorb the same volume of PBS as the sample based only on alginate [10]. Therefore, with increasing clay concentration in the alginate matrix, the swelling degree decreases (Figure 7). Also, a statistical significance of the results is presented in Figure 7.

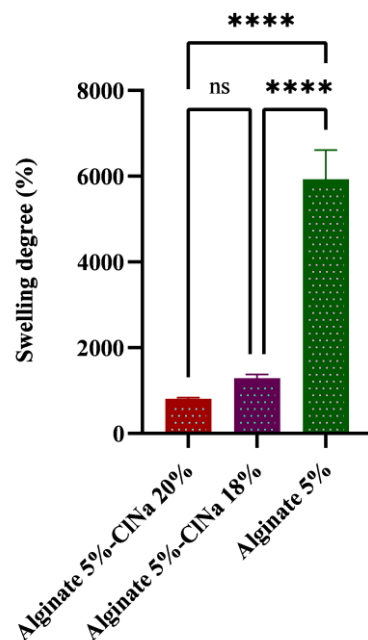


Figure 7. Swelling ratio and of alginate and nanocomposites-based hydrogel with different concentration of clay. Statistical significance: ns  $p < 0.5$ ; \*\*\*\*  $p < 0.0001$

### 3.4. Mechanical properties

Mechanical tests were performed on the equilibrium swelled samples. Both alginate and alginate-clay composite samples presented a dominant elastic behavior rather than viscous character, with a  $G' > G''$ , parameters which suggest that all these samples behaved as crosslinked hydrogels.  $G'$  decreases both with the introduction of clay into the alginate matrix but also with the increase of the clay concentration (Figure 9). This behavior was explained by the introduction of additional pores in alginate matrix. The more porous the material, the lower the mechanical properties. Also, these results have a statistical significance presented in Figure 9.

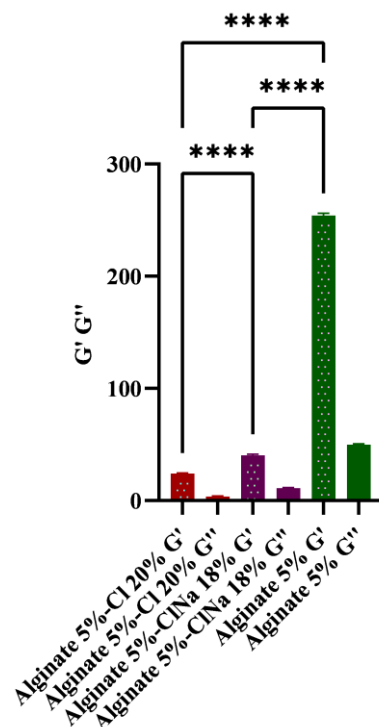


Figure 8. Storage and loss moduli determined by nanoindentation on equilibrium swollen samples. Statistical significance: \*\*\*\*  $p < 0.0001$ .

### 3.5 Thermogravimetric analysis (TGA)

TGA was used to indicate the thermal stability of the samples and to demonstrate the inclusion of montmorillonite into the alginate matrix. According to the TGA results summarized in Figure 10, alginate-clay beads showed a slight improvement of thermal stability compared to alginate beads. This improvement was attributed to the inorganic filler that caused a higher thermal stability of the samples. Also, the improvement in the thermal stability was explained by the strong interactions between clay and alginate matrix. Also, the residue at 700 °C increased from 46% for the blank sample to 72-73%

for the composite samples indicated that clay was perfectly incorporated into the biopolymeric matrix and did not migrate in the  $\text{CaCl}_2$  solution during the crosslinking step.

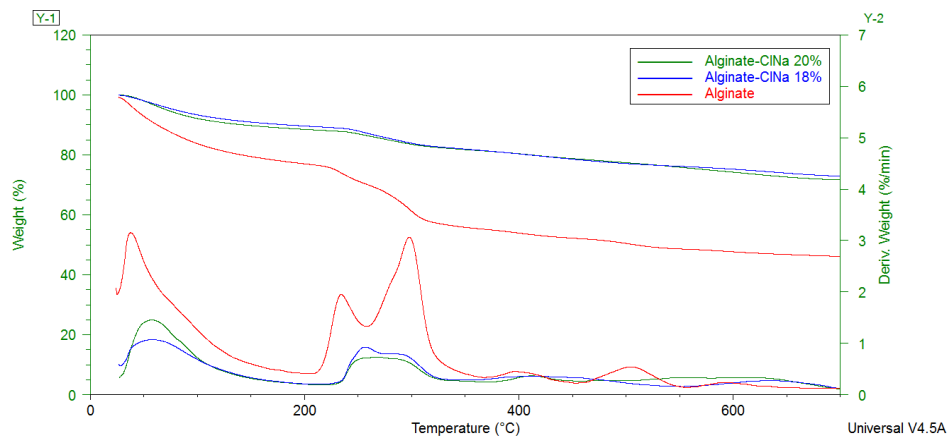


Figure 9. Thermogravimetric analysis of the alginate and nanocomposite samples.

#### 4. Conclusions

A composite ink that allowed to print 3D structures which maintained their shape fidelity, was successfully obtained. Alginate was chosen like raw material because of its features like shear thinning behavior, low cost, biocompatibility, and fast gelation. Clay was introduced in alginate matrix in order to improve its viscosity and to obtain printable inks.

FTIR and TGA analyses validate the inclusion of montmorillonite in the alginate matrix. Printability studies have shown that as the clay concentration increases, the stability of the printed structures improves. SEM analysis showed an increase in the apparent porosity of the material with the increase of clay concentration in the alginate matrix.

According to the obtained results, the nanocomposite ink based on 20% alginate-clay can be a suitable material for the achievement of 3D printed scaffolds with potential application in the domain of regenerative medicine.

#### Acknowledgments:

This work was supported by a grant of the Romanian National Authority for Scientific Research and Innovation, CNCS/CCCDI-UEFISCDI, project number PN-III-P2-2.1-PED-2019-4216, within PNCDI III. The 3D printing experiments were possible due to European Regional Development Fund through Competitiveness Operational Program 2014-2020, Priority axis 1, ID P\_36\_611, MySMIS code 107066, INOVABIOMED.

## R E F E R E N C E S

- [1]. *Leu Alexa R, Iovu H, Ghitman J, Serafim A, Stavarache C, Marin MM, Ianchis R.* 3D-Printed Gelatin Methacryloyl-Based Scaffolds with Potential Application in Tissue Engineering. *Polymers (Basel.)*, 2021 Feb 27
- [2]. *Jun, Y., Mengling Y., Yancheng, W., Jianzhong, F., and Hairui, S.*, 3D bioprinting of low concentration cell-laden gelatin methacrylate (GelMA) bioinks with two-step crosslinking strategy, *ACS Applied Materials & Interfaces*, 2018
- [3]. *Echave, M.C., Sánchez P. , Pedraz J.L., Orive G.*, Progress of gelatin-based 3D approaches for bone regeneration *Journal of Drug Delivery Science and Technology* ,Volume 42, December 2017, Pages 63-74
- [4]. *Mina Rajabi, Michelle McConnell, Jaydee Cabral, M. Azam Ali*, Chitosan hydrogels in 3D printing for biomedical applications, *Carbohydrate Polymers*, Volume 260, 2021
- [5]. *Xu Zhang, Jianlei Wang, Tianxi Liu*, 3D printing of polycaprolactone-based composites with diversely tunable mechanical gradients via multi-material fused deposition modeling, *Composites Communications*, Volume 23, 2021
- [6]. *Qiongqiong Liu, Qingtao Li, Sheng Xu, Qiujuan Zheng and Xiaodong Cao*, Preparation and Properties of 3D Printed Alginate–Chitosan Polyion Complex Hydrogels for Tissue Engineering, Received: 9 May 2018; Accepted: 9 June 2018; Published: 14 June 2018
- [7]. *Sudipto Datta, Ranjit Barua and Jonali Das*, Importance of Alginate Bioink for 3D Bioprinting in Tissue Engineering and Regenerative Medicine Submitted: May 10th 2019Reviewed: November 8th 2019Published: December 9th 2019
- [8]. *Giovanni Falcone, Marilena Saviano, Rita P. Aquino, Pasquale Del Gaudio, Paola Russo*, Coaxial semi-solid extrusion and ionotropic alginate gelation: A successful duo for personalized floating formulations via 3D printing, *Carbohydrate Polymers*, Volume 260, 2021.
- [9]. *Mahdiyar Shahbazi, Henry Jäger, Seyed Javad Ahmadi, Monique Lacroix*, Electron beam crosslinking of alginate/nanoclay ink to improve functional properties of 3D printed hydrogel for removing heavy metal ions, *Carbohydrate Polymers*, Volume 240, 2020, 116211, ISSN 0144-8617, <https://doi.org/10.1016/j.carbpol.2020.116211>.
- [10]. *Alexa, R.L.; Iovu, H.; Trica, B.; Zaharia, C.; Serafim, A.; Alexandrescu, E.; Radu, I.-C.; Vlasceanu, G.; Preda, S.; Ninciuleanu, C.M.; Ianchis, R.* Assessment of Naturally Sourced Mineral Clays for the 3D Printing of Biopolymer-Based Nanocomposite Inks. *Nanomaterials* **2021**,
- [11]. *Gaharwar, A.K.; Cross, L.M.; Peak, C.W.; Gold, K.; Carrow, J.K.; Brokesh, A.; Singh, K.A.* 2D Nanoclay for Biomedical Applications: Regenerative Medicine, Therapeutic Delivery, and Additive Manufacturing. *Adv. Mater.* **2019**
- [12]. *Ahlfeld, T.; Cidonio, G.; Kilian, D.; Duin, S.; Akkineni, A.R.; Dawson, J.I.; Yang, S.; Lode, A.; Oreffo, R.O.C.; Gelinsky, M.* Development of a Clay Based Bioink for 3D Cell Printing for Skeletal Application. *Biofabrication* **2017**
- [13]. *Mieszawska, A.J.; Llamas, J.G.; Vaiana, C.A.; Kadakia, M.P.; Naik, R.R.; Kaplan, D.L.* Clay Enriched Silk Biomaterials for Bone Formation. *Acta Biomaterialia* **2011**
- [14]. *Jayrajsinh, S.; Shankar, G.; Agrawal, Y.K.; Bakre, L.*, Montmorillonite Nanoclay as a Multifaceted Drug-Delivery Carrier: A Review. *Journal of Drug Delivery Science and Technology* **2017**
- [15]. *Jafarbeglou, M.; Abdouss, M.; Shoushtari, A.M.; Jafarbeglou, M.* Clay Nanocomposites as Engineered Drug Delivery Systems. *RSC Adv.* **2016**
- [16]. *H. M. Ismail, S. Zamani, M. A. Elrayess, W. Kafienah and H. M. Younes*, New Three-Dimensional Poly(decanediol-co-tricarballylate) Elastomeric Fibrous Mesh Fabricated by

Photoreactive Electrospinning for Cardiac Tissue Engineering Applications, Polymers, 19 April 2018

- [17]. *Ianchis, R. et al.*, Novel Hydrogel-Advanced Modified Clay Nanocomposites as Possible Vehicles for Drug Delivery and Controlled Release. *Nanomaterials* **7**, 443 (2017).
- [18]. García-Guzmán, P. *et al.*, Characterization of hybrid microparticles/Montmorillonite composite with raspberry-like morphology for Atorvastatin controlled release. *Colloids Surf B Biointerfaces* **167**, 2018
- [19]. *Wadell, H.*, Volume, Shape, and Roundness of Rock Particles. *J. Geol.* **1932**, 40, pp 443–451